

**Electronic Supporting Information
for
Dynamic structural changes of pentacopper(II) chains supported by
 \mathbf{N}_6 -donor ligands†**

*Yukie Takemura,^a Takayuki Nakajima^a Tomoaki Tanase^{*a} Miho Usuki,^a
Hiroe Takenaka,^a Eri Goto^a and Masahiro Mikuriya^b*

Experimental and spectral data for H₂panapy

Experimental and spectral data for complexes 1-4

Figure S1. ORTEP plot of **1** and selected bond distances and angles

Figure S2. ORTEP plot of **2** and selected bond distances and angles

Figure S3. ORTEP plot for the complex cation of **3** and selected bond distances and angles

Figure S4. ORTEP plot for the complex cation of **4** and selected bond distances and angles

Figure S5. Temperature dependent magnetic susceptibility data and effective magnetic moments for **1** and **3** together with curve-fitting results

Figure S6. EPR spectrum of **1** at room temperature

^a Department of Chemistry, Faculty of Science, Nara Women's University, Kitauoya-higashi-machi, Nara 630-8506, Japan. Fax: +81 742 203847; Tel: +81 742 203399; E-mail: tanase@cc.nara-wu.ac.jp

^b Department of Chemistry, School of Science and Technology, Kwansei Gakuin University, 2-1 Gakuen, Sanda-shi, Hyogo 699-1337, Japan.

Experimental and spectral data for H₂panapy

Portions of 2,7-dichloro-1,8-naphthyridine (0.745g, 3.74 mmol), *t*BuOK (2.5 g, 22.5 mmol) and 2-aminopyridine (1.47g, 15.6 mmol) were dissolved in dry THF (40 mL) under nitrogen atmosphere and placed into a stainless steel tube. The sealed stainless steel tube was heated at 80 °C for ca. 90 h and then cooled to room temperature. The resultant reaction mixture was poured into ice water, and its pH was adjusted at 7. The organic components were extracted with 30 mL of dichloromethane (10 times) and the extract was concentrated to ca. 20 mL. After addition of Et₂O (20 mL), the mixture was allowed to stand at 2 °C to give yellow-brown powder of 2,7-bis(2-pyridylamino)-1,8-naphthyridine·0.5H₂O (H₂panapy·0.5H₂O) in 56 % yield (680 mg), which was washed with diethyl ether and dried under vacuum. ESI-MS: m/z 315.1508 (315.1353 calcd for MH⁺), Anal. Calcd for C₁₈H₁₅N₆O_{0.5}: C, 66.86; H, 4.68; N, 25.99 %, Found C, 66.98; H 4.79; N, 26.28 %, IR (KBr): ν ~ 1617 (m), 1591 (m), 1518 (s), 1479 (s), 1433 (s), 1339 (s), 1233 (m), 1141 (m), 773 (m) cm⁻¹, ¹H NMR (300 MHz, DMSO-*d*₆): δ 6.97 (dd, 2H, *J* = 5.3 Hz, *J'* = 6.8 Hz), 7.65 (d, 2H, *J* = 8.7 Hz), 7.78 (ddd, 2H, *J* = *J'* = 7.9 Hz, *J''* = 2.0 Hz), 8.03 (d, 2H, *J* = 8.4 Hz), 8.26 (d, 2H, *J* = 9.3 Hz), 8.29 (dd, 2H, *J* = 5.4 Hz, *J'* = 1.8 Hz).

Experimental and spectral data for complexes 1-4

Procedures for complexes **3** and **4** were carried out under nitrogen atmosphere using standard Schlenk techniques.

1: To a suspension of H₂panapy·0.5H₂O (201 mg, 0.639 mmol) in *n*-butanol (23 mL), potassium *tert*-butoxide (420 mg, 3.74 mmol) and CuCl₂ (267 mg, 1.99 mmol) were added and the reaction mixture was stirred at 160 °C for 1 h. After removal of the solvent under reduced pressure, the residue was extracted with dichloromethane (300 mL). The brown extract was concentrated and was kept at room temperature to afford brown crystals of **1**·0.75CH₂Cl₂. Yield 179 mg, 66 %. Anal. Calcd for C_{72.75}H_{49.5}N₂₄Cl_{3.5}Cu₅: C, 51.35; H, 2.93; N, 19.75 %, Found C, 51.43; H 2.88; N, 19.74 %; IR (KBr pellet): ν ~ 1591 (s), 1551 (m), 1503 (s), 1473 (s), 1426 (s), 1360 (s), 1272 (m), 1146 (s), 1014 (m), 954 (m), 788 (m), 763 (m) cm⁻¹; UV-Vis (CH₂Cl₂) [λ _{max}; nm (ϵ ; Lcm⁻¹mol⁻¹)]: 414 (1.01 × 10⁵), 442^{sh} (4.15 × 10⁴); ESI-MS (CH₂Cl₂) *m/z*: 1602.155 (*z* = 1) (1602.064 calcd for [Cu₅Cl(panapy)₄]⁺).

2: H₂panapy·0.5H₂O (99.8 mg, 0.308 mmol), potassium *tert*-butoxide (219 mg, 1.96 mmol) and CuBr₂ (255 mg, 1.14 mmol) were mixed in *n*-butanol (20 mL) and stirred at 160 °C for 1 h to result in a brown solution. After removal of the solvent, the residue was extracted with dichloromethane (300 mL). The brown extract was concentrated and was kept at room temperature to give brown crystals of **2**. Yield 57.6 mg, 43 %. Anal. Calcd for C₇₂H₄₈N₂₄Br₂Cu₅: C 50.08, H 2.80, N, 19.47 %, Found C 49.92, H 2.92, N 19.08 %; IR (KBr pellet): ν ~ 1592 (s), 1551 (m), 1503 (s), 1473 (s), 1426 (s), 1360 (s), 1272 (m), 1146 (s), 1013 (m), 956 (m), 789 (m), 762 (m) cm⁻¹; UV-Vis (CH₂Cl₂) [λ _{max}; nm (ϵ ; Lcm⁻¹mol⁻¹)]: 415 (1.12 × 10⁵), 441^{sh} (4.76 × 10⁴); ESI-MS (CH₂Cl₂) *m/z*: 1646.071 (*z* = 1) (1646.013 calcd for [Cu₅Br(panapy)₄]⁺).

3: Complex **1**·0.75CH₂Cl₂ (20.2 mg, 0.012 mmol) and NH₄BF₄ (26.8 mg, 0.256 mmol) were suspended in dichloromethane (15 mL) and the reaction mixture was stirred at room temperature overnight to result in a green suspension. After filtration, the solution was kept at room temperature to afford brown crystals of **3**·1.25CH₂Cl₂. Yield 10.2 mg, 47 %. Anal. Calcd for C_{73.25}H_{50.5}N₂₄B₂Cl_{2.5}Cu₅F₈: C 47.64, H 2.76, N 18.20 %, Found C 47.99, H 2.96, N 17.99 %; IR (KBr pellet): ν ~ 1590 (s), 1553 (m), 1506 (s), 1475 (s), 1428 (s), 1362 (s), 1273 (m), 1149 (s), 1023 (m), 953 (m), 783 (m), 764 (m), 1083 (br, BF₄) cm⁻¹; UV-Vis (CH₂Cl₂) [λ_{max} ; nm (ϵ ; Lcm⁻¹mol⁻¹)]: 410 (1.34 × 10⁵), 443^{sh} (4.56 × 10⁴), 467^{sh} (2.36 × 10⁴); ESI-MS (CH₂Cl₂) *m/z*: 1654.068 (*z* = 1) (1654.099 calcd for {[Cu₅(panapy)₄](BF₄)⁺}).

4: Method A NH₄PF₆ (299 mg, 1.83 mmol) was added to a suspension of complex **1**·0.75CH₂Cl₂ (151 mg, 0.089 mmol) in dichloromethane (15 mL) and the reaction mixture was stirred at room temperature overnight to give a green suspension. After filtration, the solution was kept at room temperature to afford brown crystals of **4**·0.5CH₂Cl₂. Yield 11.3 mg, 7 %. Anal. Calcd for C_{72.5}H₄₉N₂₄P₂ClCu₅F₁₂: C 45.84, H 2.60, N 17.70 %, Found C 45.91, H 2.53, N 17.33 %; IR (KBr pellet): ν ~ 1591 (s), 1555 (m), 1507 (s), 1476 (s), 1432 (s), 1365 (s), 1274 (m), 1150 (s), 1023 (m), 955 (m), 783 (m), 765 (m), 846(s, PF₆) cm⁻¹; UV-Vis (CH₂Cl₂) [λ_{max} ; nm (ϵ ; Lcm⁻¹mol⁻¹)]: 413 (1.06 × 10⁵), 443^{sh} (3.64 × 10⁴), 467^{sh} (1.90 × 10⁴); ESI-MS (CH₂Cl₂) *m/z*: 1712.218 (*z* = 1) (1712.060 calcd for {[Cu₅(panapy)₄](PF₆)⁺}).

Method B AgPF₆ (23.0 mg, 0.091 mmol) was added to a suspension of complex **1**·0.75CH₂Cl₂ (50.7 mg, 0.030 mmol) in dichloromethane (10 mL) and the reaction mixture was stirred at room temperature overnight to afford a green suspension. After filtration, the solution was kept at room temperature to afford brown crystals of **4**·0.5CH₂Cl₂. Yield 11.6 mg, 20 %.

Figure S1. ORTEP plots of **1**. Selected distances [Å] and angles [°]: Cu(1)…Cu(2) 2.6064(6), Cu(2)…Cu(3) 3.1124(5), Cu(3)…Cu(4) 3.1276(5), Cu(4)…Cu(5) 2.6126(6), Cu(1)–Cl(1) 2.5395(13), Cu(1)–N(11) 2.073(3), Cu(1)–N(21) 2.050(3), Cu(1)–N(31) 2.067(3), Cu(1)–N(41) 2.030(3), Cu(2)–N(12) 1.960(3), Cu(2)–N(22) 2.040(3), Cu(2)–N(32) 1.981(3), Cu(2)–N(42) 2.088(3), Cu(2)…N(33) 2.655(3), Cu(2)…N(43) 2.412(3), Cu(3)–N(13) 2.072(3), Cu(3)–N(23) 2.063(3), Cu(3)–N(34) 2.073(3), Cu(3)–N(44) 2.068(3), Cu(3)…N(24) 2.524(3), Cu(3)…N(33) 2.494(3), Cu(4)–N(15) 2.077(3), Cu(4)–N(25) 1.986(3), Cu(4)–N(35) 2.035(3), Cu(4)–N(45) 1.970(3), Cu(4)…N(14) 2.432(3), Cu(4)…N(24) 2.640(3), Cu(5)–CL(2) 2.5571(12), Cu(5)–N(16) 2.023(4), Cu(5)–N(26) 2.069(3), Cu(5)–N(36) 2.061(3), Cu(5)–N(46) 2.086(3); Cl(1)–Cu(1)–Cu(2) 174.97(4), Cu(1)–Cu(2)–Cu(3) 163.04(2), Cu(2)–Cu(3)–Cu(4) 174.037(19), Cu(3)–Cu(4)–Cu(5) 164.29(2), Cl(2)–Cu(5)–Cu(4) 175.02(3).

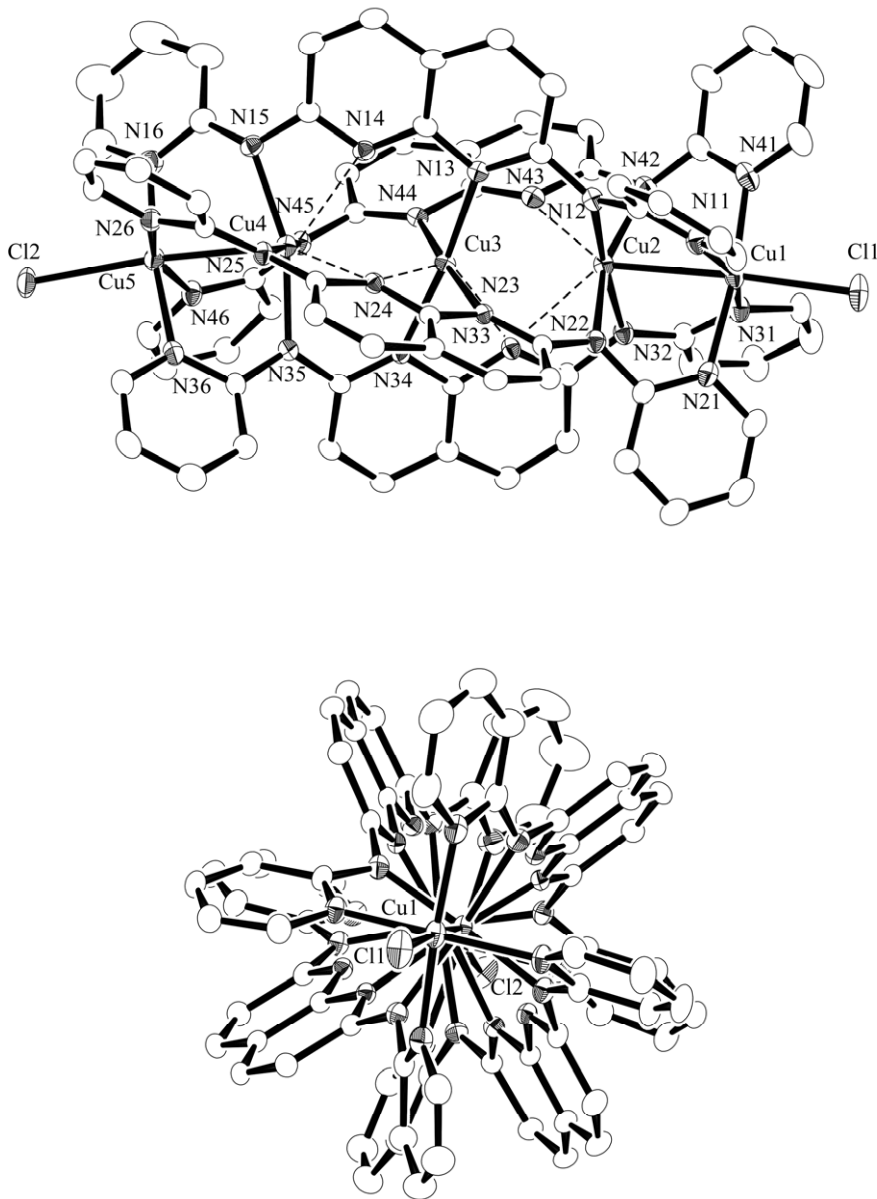


Figure S2. ORTEP plots of **2**. Selected distances [Å] and angles [°]: Cu(1)…Cu(2) 2.5995(18), Cu(2)…Cu(3) 3.1208(18), Cu(3)…Cu(4) 3.1173(17), Cu(4)…Cu(5) 2.6026(17), Cu(1)–Br(1) 2.6954(18), Cu(1)–N(11) 2.056(9), Cu(1)–N(21) 2.080(9), Cu(1)–N(31) 2.015(10), Cu(1)–N(41) 2.081(10), Cu(2)–N(12) 2.012(8), Cu(2)–N(22) 1.986(10), Cu(2)–N(32) 2.070(9), Cu(2)–N(42) 1.956(9), Cu(2)…N(23) 2.653(9), Cu(2)…N(33) 2.438(8), Cu(3)–N(13) 2.068(8), Cu(3)–N(24) 2.081(9), Cu(3)–N(34) 2.075(8), Cu(3)–N(43) 2.065(9), Cu(3)…N(14) 2.513(9), Cu(3)…N(23) 2.516(9), Cu(4)–N(15) 1.977(9), Cu(4)–N(25) 2.057(9), Cu(4)–N(35) 1.956(9), Cu(4)–N(45) 2.089(9), Cu(4)…N(14) 2.642(8), Cu(4)…N(44) 2.412(9), Cu(5)–Br(2) 2.7391(19), Cu(5)–N(16) 2.062(9), Cu(5)–N(26) 2.042(9), Cu(5)–N(36) 2.066(10), Cu(5)–N(46) 2.025(10); Br(1)–Cu(1)–Cu(2) 176.74(6), Cu(1)–Cu(2)–Cu(3) 164.02(6), Cu(2)–Cu(3)–Cu(4) 173.95(5), Cu(3)–Cu(4)–Cu(5) 162.44(6), Br(2)–Cu(5)–Cu(4) 177.04(7).

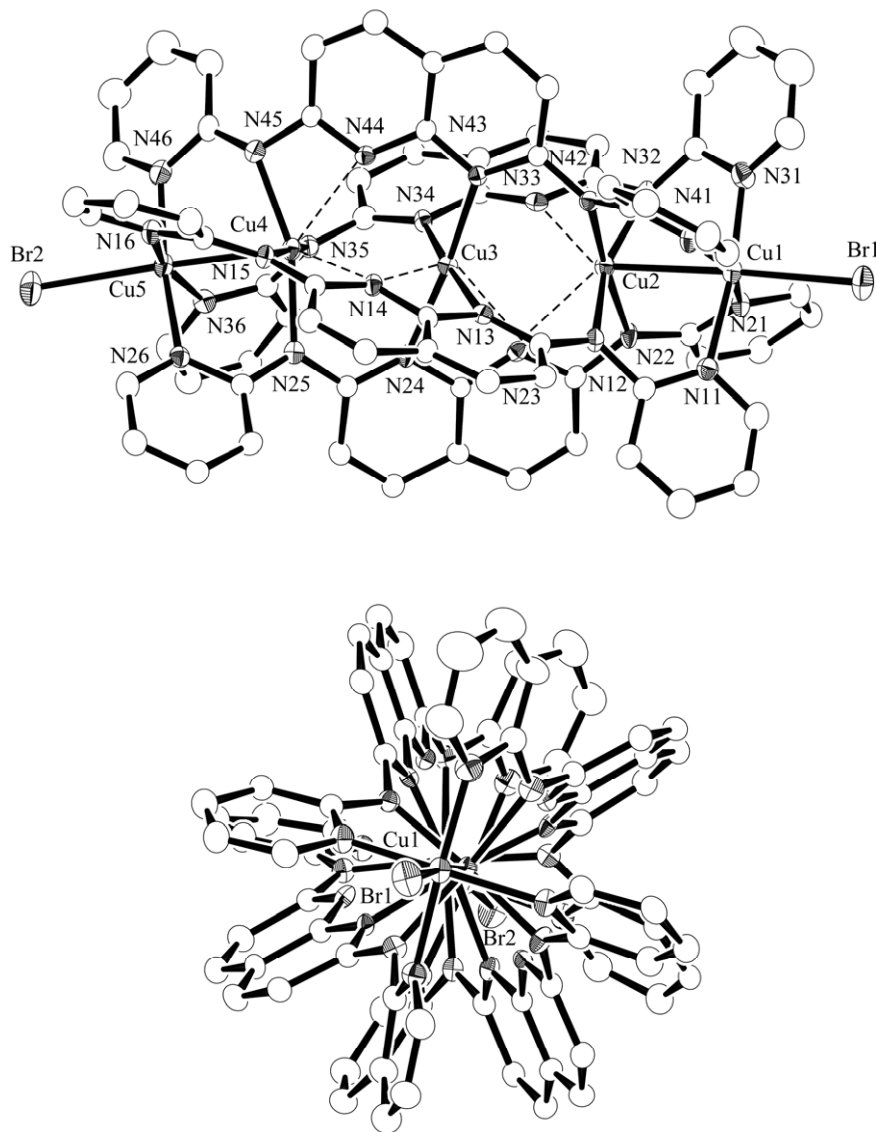


Figure S3. ORTEP plots for the complex cation of **3**. Selected distances [Å] and angles [°]: Cu(1)…Cu(2) 2.6537(18), Cu(2)…Cu(3) 2.6967(16), Cu(3)…Cu(4) 2.6538(15), Cu(4)…Cu(5) 2.6338(17), Cu(1)–N(11) 2.025(8), Cu(1)–N(21) 1.965(9), Cu(1)–N(31) 2.243(8), Cu(1)–N(32) 2.182(8), Cu(1)–N(41) 2.014(10), Cu(2)–N(12) 1.998(9), Cu(2)–N(22) 2.170(9), Cu(2)–N(23) 2.283(9), Cu(2)–N(33) 2.029(8), Cu(2)–N(42) 2.005(9), Cu(2)…N(32) 2.737(8), Cu(3)–N(13) 2.114(9), Cu(3)–N(24) 2.023(9), Cu(3)–N(34) 2.019(10), Cu(3)–N(43) 1.988(8), Cu(3)…N(14) 2.407(9), Cu(3)…N(23) 2.597(8), Cu(4)–N(15) 2.048(10), Cu(4)–N(25) 2.013(8), Cu(4)–N(35) 1.964(10), Cu(4)–N(44) 2.036(8), Cu(4)…N(14) 2.429(9), Cu(4)…N(45) 2.631(7), Cu(5)–N(16) 1.987(11), Cu(5)–N(26) 2.032(8), Cu(5)–N(36) 2.003(10), Cu(5)–N(45) 2.277(8), Cu(5)–N(46) 2.112(8); Cu(1)–Cu(2)–Cu(3) 167.39(8), Cu(2)–Cu(3)–Cu(4) 172.68(6), Cu(3)–Cu(4)–Cu(5) 169.81(8).

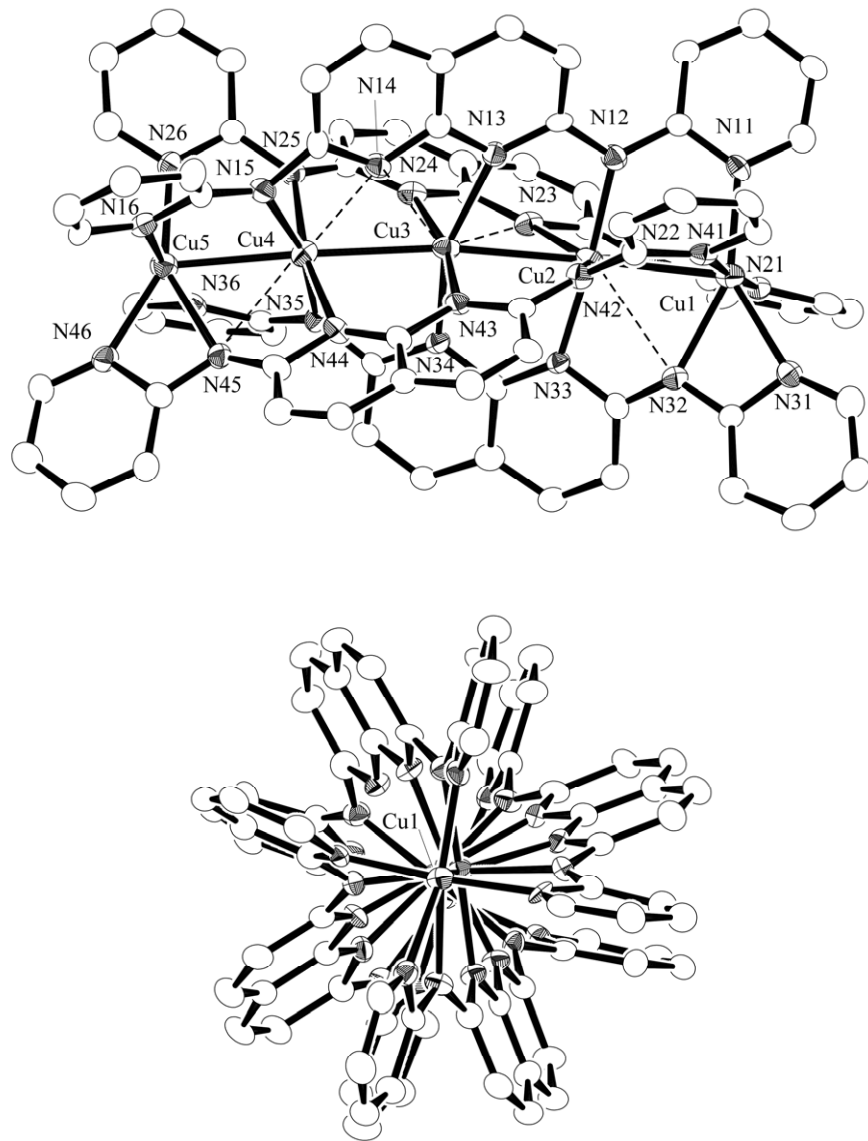


Figure S4. ORTEP plots for the complex cation of of 4. Selected distances [\AA] and angles [$^\circ$]: Cu(1)…Cu(2) 2.6229(16), Cu(2)…Cu(3) 2.6854(14), Cu(3)…Cu(4) 2.7155(13), Cu(4)…Cu(5) 2.6325(14), Cu(1)–N(11) 2.124(8), Cu(1)–N(12) 2.238(5), Cu(1)–N(21) 1.967(7), Cu(1)–N(31) 2.015(7), Cu(1)–N(41) 2.006(7), Cu(2)–N(13) 2.034(5), Cu(2)–N(22) 2.088(7), Cu(2)–N(32) 2.004(6), Cu(2)–N(42) 1.976(7), Cu(2)…N(12) 2.618(8), Cu(2)…N(23) 2.429(8), Cu(3)–N(14) 2.015(6), Cu(3)–N(24) 2.129(8), Cu(3)–N(33) 2.067(6), Cu(3)–N(43) 2.024(7), Cu(3)…N(23) 2.468(6), Cu(3)…N(34) 2.497(6), Cu(4)–N(15) 1.972(7), Cu(4)–N(25) 2.001(8), Cu(4)–N(35) 2.067(7), Cu(4)–N(44) 2.041(8), Cu(4)…N(34) 2.380(6), Cu(4)…N(45) 2.621(5), Cu(5)–N(16) 2.005(7), Cu(5)–N(26) 2.000(8), Cu(5)–N(36) 1.978(7), Cu(5)–N(45) 2.236(9), Cu(5)–N(46) 2.146(5); Cu(1)–Cu(2)–Cu(3) 170.87(6), Cu(2)–Cu(3)–Cu(4) 172.67(5), Cu(3)–Cu(4)–Cu(5) 168.32(6).

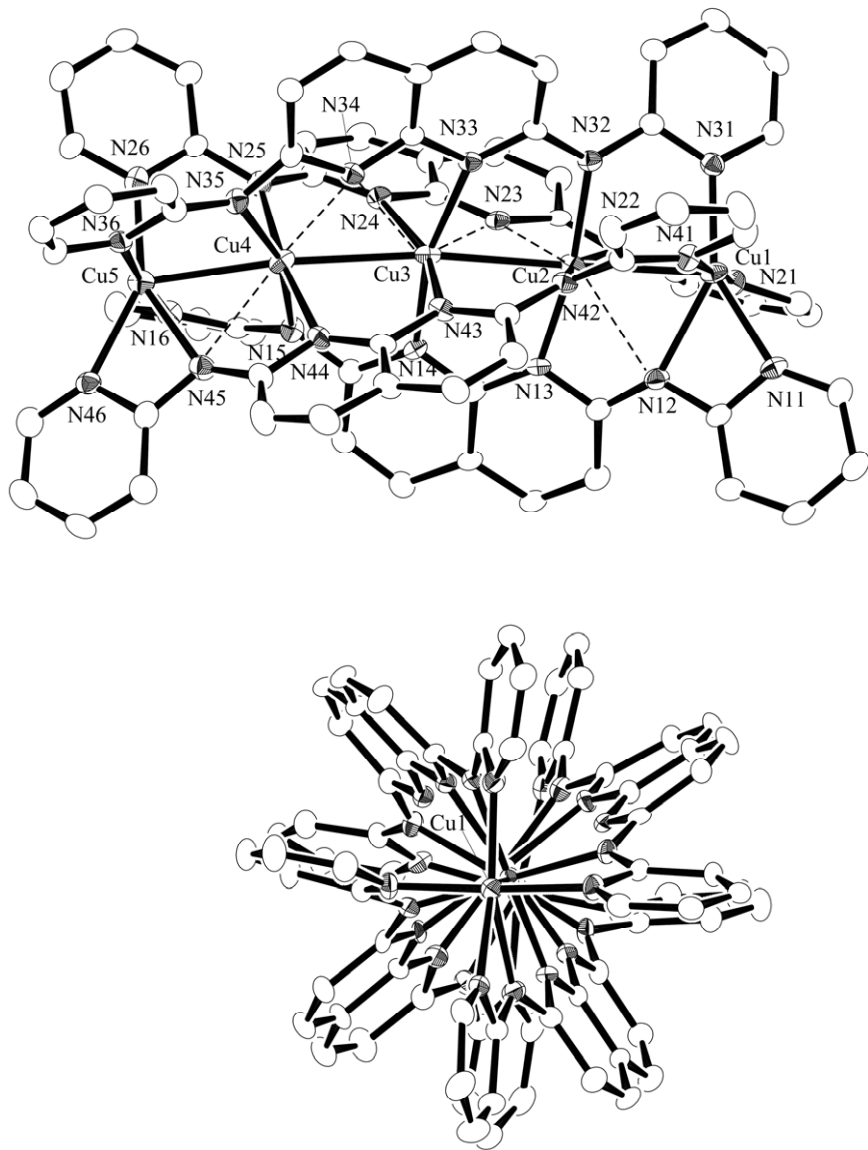
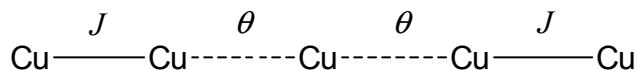
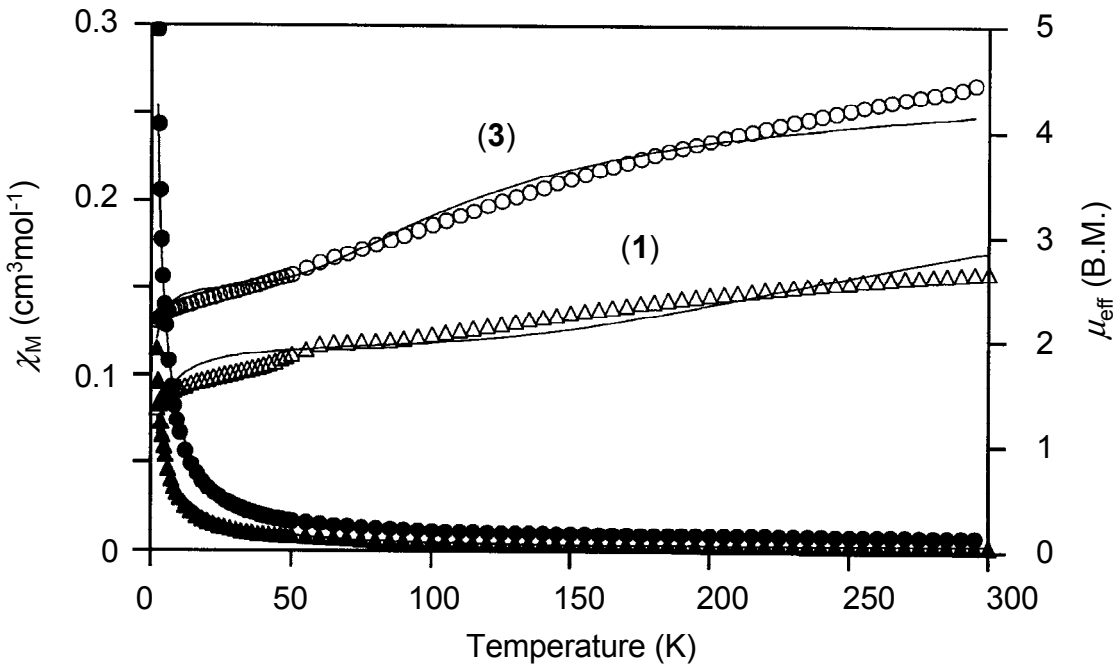


Figure S5. Temperature dependent magnetic susceptibility data and effective magnetic moments for **1** (\blacktriangle , \triangle) and **3** (\bullet , \circ). The solid lines are best fits with equation (1).^{a)}



$$\chi_M = \frac{4N g^2 \beta^2}{kT} [3 + \exp(-2J/kT)]^{-1} + C/(T - \theta) + 5N\alpha \quad (\text{eq. 1})$$

$$N\alpha = 60 \times 10^{-6} \text{ cm}^3\text{mol}^{-1}$$

For **1**: $g = 2.1$ (fixed),^b $J = -252 \text{ cm}^{-1}$, $\theta = -4.2 \text{ K}$, $C = 0.48 \text{ cm}^3\text{mol}^{-1}$

For **3**: $g = 2.1$ (fixed),^b $J = -86 \text{ cm}^{-1}$, $\theta = -1.2 \text{ K}$, $C = 0.82 \text{ cm}^3\text{mol}^{-1}$

- a) M. Mikuriya, H. Azuma, R. Nukada, Y. Sayama, K. Tanaka, J. -W Lim and M. Handa, *Bull. Chem. Soc. Jpn.*, 2000, **73**, 2493-2498.
 b) g value is fixed at 2.10 on the basis of the EPR spectrum of **1** (see Figure S6).

Figure S6. X-band powder EPR spectrum of **1** measured by a Jeol JES-TE100 ESR spectrometer at room temperature, showing an unsymmetrical and broad absorption at $g = 2.10$.

